

# Modeling of PAH Formation in Laminar Premixed Benzene-Air-Flames

E. Goos<sup>\*</sup>, M. Braun-Unkhoff and P. Frank  
Institut für Verbrennungstechnik  
Deutsches Zentrum für Luft- und Raumfahrt e.V. (DLR)  
Pfaffenwaldring 38-40  
70569 Stuttgart, Germany

## Abstract

In the combustion of larger hydrocarbon fuels, polycyclic aromatic hydrocarbons (PAH) are formed and have been identified as key precursors for soot particles. In the present work, the predictions of formation and growth of PAHs, using a comprehensive gas phase reaction model, are compared with species profiles measured in laminar premixed benzene-air-flames of different C/O-ratios at atmospheric pressure. Main growth routes leading from the formation of low mass hydrocarbons up to six ring aromatics have been identified. In particular, attention was put on reliable prediction of 3- to 4-ring aromatics like phenanthrene and pyrene, as these species are considered as starting points for particle inception by coalescence in current physicochemical soot models. Additionally, measured soot volume profiles were simulated by combining the gas phase reaction mechanism with a current mechanistic particle model.

## Introduction

Aromatics and polycyclic aromatic hydrocarbons (PAH) are formed in the combustion of hydrocarbon fuels (e.g. kerosene). They are of particular concern because of their potentially adverse health effects. Furthermore, they have been identified as key precursors of soot particles. Besides a model describing the formation, growth and oxidation of soot particles, a soot model must also comprise a comprehensive gas phase fuel break-up and PAH formation reaction mechanism. Former shock tube experiments and investigations of flames, in particular at high pressures, have shown the importance of PAH growth sub models on soot particle inception and on calculated soot volume fractions [1, 2]. As particle inception is described in nearly all current soot models exclusively by coagulation of large mass PAHs, the influence of different PAHs on the onset and the amount of soot has to be investigated systematically. Modeling studies [3] reveal that only a few PAH species which appear in maximum concentrations must be considered in the current soot models for simulation of particle inception.

## Specific Objectives

At present, detailed modeling of soot formation and destruction is performed by using a relatively large gas phase reaction mechanism coupled with a mechanistic soot model.

## Gas phase reaction mechanism

To describe both the initial hydrocarbon pyrolysis and oxidation and the growth of polyaromatic species, the reaction mechanism from [4] which comprises reactions of aromatic species up to pyrene, too, was used as base model. Its C<sub>1</sub>- to C<sub>4</sub>-sub model, which was updated by taking into account recent results (see for example ref. [3]), was validated by modelling the concentration profiles measured in a laminar, sooting ethene/oxygen/argon flame operated at atmospheric pressure [5]. In particular, the used mechanism reproduces the experimental values for the C<sub>1</sub>- and C<sub>2</sub>-species' concentrations very well.

Furthermore, the mechanism was enlarged with reactions describing combinative growth steps of aromatic species as proposed recently in ref. [6], and the formation of species with up to 30 carbon atoms [7]. Also, results of shock tube experiments for reactions of small aromatics such as cyclopentadiene, toluene, phenol, phenylacetylene including their radicals, and the propargyl radical [9] were taken into account (see ref. 2, 3). In particular, the branching ratio of reactions with aromatic species turned out to be of importance with respect to formation of soot precursors. For example, the recombination of propargyl radicals leads predominantly to the formation of benzene and not to phenyl and H-atoms [9]; furthermore, propargyl radicals can react with benzyl, which is produced by pyrolysis of benzene, leading to naphthalene [e.g. 10].

---

<sup>\*</sup> Corresponding author: Elke.Goos@dlr.de

Associated Web site: <http://www.dlr.de/VT/>

Proceedings of the European Combustion Meeting 2005

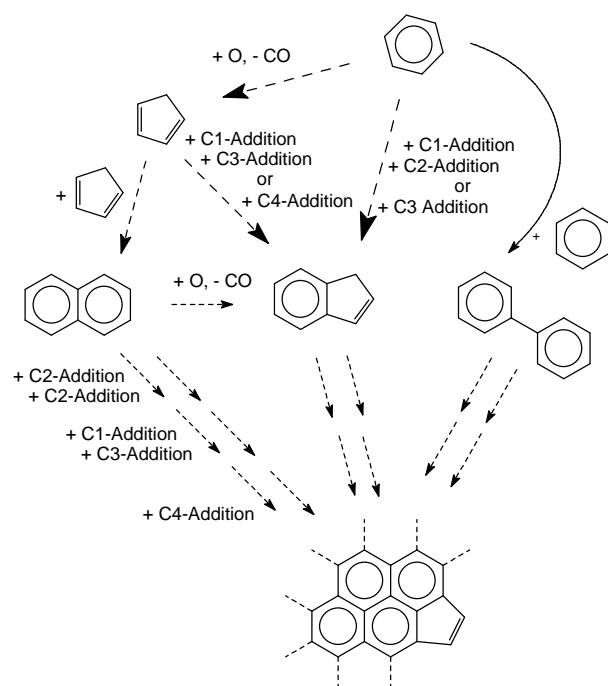


Figure 1: Principal reaction scheme for initial PAH formation.

The updated and refined PAH growth submodel contains about 96 species up to benzopyrene ( $C_{20}H_{12}$ ) and 280 elementary reaction steps. Figure 1 depicts the principal starting routes of the model. Dominant pathways are for example (i) the hydrogen-abstraction-carbon-addition (HACA or C2 Addition) path, (ii) the combinative growth path, which leads to the formation of biphenyl by the reaction of benzene and phenyl, and (iii) the cyclopentadienyl recombination producing naphthalene, and additional routes to form indene which then can grow by further reactions with cyclopentadienyl.

Figure 2 depicts the principal growth routes of the higher mass aromatics in the refined PAH sub model which again comprises the classical hydrogen-abstraction-carbon-addition (HACA or C2-Addition) path and also the OH oxidative pathway, H abstraction and recombination reactions. Only the HACA and isomerisation routes are shown in figure 2, starting with phenanthrene. It is to be seen that – according to this simplified scheme – phenanthrene and pyrene can be considered as bottlenecks for the formation of the higher mass PAHs which are found in comparably high concentrations in the experiments (see Results and Discussion).

The complete mechanism with a total of about 670 reactions and 170 species was used to describe in detail the evolution of the gaseous species up to the starting point of the particle inception model. Most of the gas phase reactions are treated as reversible with rate coefficients for the reverse reactions evaluated from the respective equilibrium constant. Only a few reaction steps, representing preferentially isomerization reactions, are considered with separate rate coefficient expressions for forward and reverse direction.

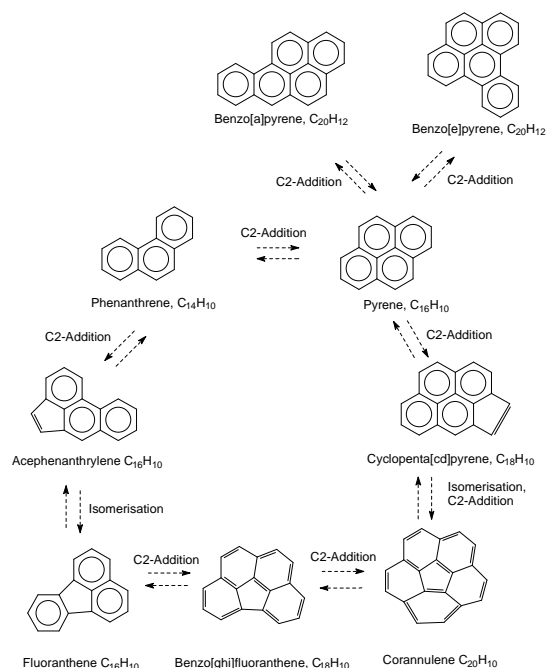


Figure 2: Principal reaction scheme for principal growth routes of the higher mass PAHs.

The experimental data base for the rate constants in the PAH mechanism is extremely poor. Therefore, most of the data had to be estimated from the comparison with similar reactions of smaller aromatics like e.g. splitting off a methyl group after H-atom attack on a methylated PAH. The thermodynamic data of the PAH species – which are taken from ref. [11] – are of large importance for the calculation of the reverse rate constants. However, these thermodynamic data often are not available and have to be calculated by quantum mechanical methods, which sometimes can lead to relatively large errors.

### Mechanistic soot model

For modeling the measured soot concentration, the original soot model of Frenklach and Wang [1], which uses the method of moments for describing the PAH and soot particle dynamics, was modified. Detailed PAH chemistry was implemented, and all PAHs with masses larger than phenanthrene or pyrene were allowed to undergo coagulation. Further growth of the particles occurs by coagulation of the particles, for which pressure dependence was included, and by surface growth, predominantly controlled by reactions of active surface sites with acetylene and PAH. Finally, decrease in the particle size is described by reactions of the surfaces with OH and  $O_2$ .

An essential quantity for surface mass growth in the model is the steric parameter  $\alpha$ , which accounts for the fraction of surface sites available for corresponding reactions and which is a function of temperature and particle age, respectively [14].

## Results and Discussion

For comparison with calculated data, experimental literature values from premixed laminar benzene flames [12] were used. The calculation of the concentration versus height profiles has been executed with the 1-dimensional PREMIX-code of the CHEMKIN-package [13] and the given temperature profiles, which were obtained by thermocouple measurements and corrected to radiation losses.

### Slightly sooting benzene/air flame, C/O = 0.72:

#### Small Species

The comparison between model calculation and experimental data in Figure 3 shows that the concentrations of the combustion products CO, CO<sub>2</sub> and acetylene – the most important gaseous component for PAH and surface growth – are reproduced well by the detailed gas phase reaction model.

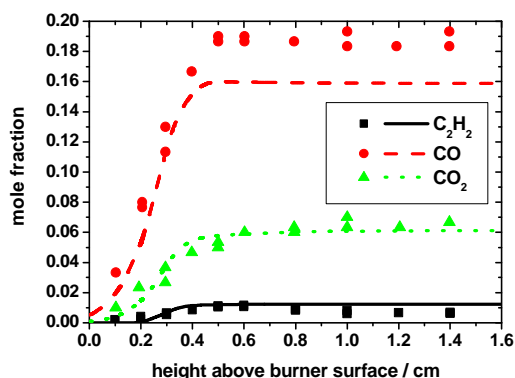


Figure 3: Comparison between model prediction (curves) and experimental data (symbols) for CO, CO<sub>2</sub> and C<sub>2</sub>H<sub>2</sub> in a premixed laminar atmospheric benzene/air flame, C/O = 0.72 [12].

#### Aromatic species

The comparison between measured and predicted concentration profiles of low mass PAHs is displayed in Fig. 4. The measured concentrations of the fuel benzene are predicted well by the reaction model as the shape of the biphenyl concentration profile, which is not shown in this graph.

Regarding naphthalene, both the maximum of the concentration and the concentration level in the post reaction zone are reproduced well. For phenanthrene, which is generally considered to play a central role for the growth of the PAHs, the concentration profile is reproduced well, besides some over prediction considering the height of the maximum. The concentration profile for acenaphthalene which is not shown in the picture gives also good agreement with the prediction. The initial rise of the experimental data for pyrene up to the maximum is simulated well, but the model calculation overpredicts the data in the post reaction zone regime by about one order of magnitude.

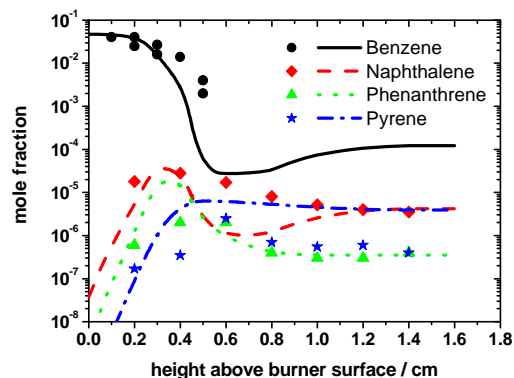


Figure 4: Comparison between model prediction (curves) and experimental data (symbols) for low mass aromatic species in a premixed laminar atmospheric benzene/air flame, C/O = 0.72 [12].

In Figure 5, measured and calculated concentration profiles for larger mass PAHs (see also Fig. 2) are shown. Principally, the numerical prediction meets the initial rise of the experimental profiles sufficiently but overpredicts the values at higher flame heights. The calculated fluoranthene profile shows a shape similar to that of phenanthrene (Fig. 4). Same behaviour is observed for cyclpenta(c,d)pyrene (Fig. 5) and pyrene (Fig. 4), too.

It is observed that in the slightly sooting flame (C/O=0.72) the measured concentration profiles of low and of larger mass PAHs first reach a maximum around 4 - 6 mm before they decrease significantly for larger heights above burner. The concentration profiles of lower mass species and smaller aromatics show pronounced maxima which are typical for intermediate products.

The predicted concentration profiles of larger PAHs show a good agreement in the reaction zone; whereas in the post flame zone, the measured decrease is not matched, but overpredicted considerably. A possible explanation is connected to the difficulties in measuring larger PAHs' concentrations correctly due to their pronounced adsorption tendency as a result from their high boiling points. Therefore, measurements would give too low values for larger PAHs.

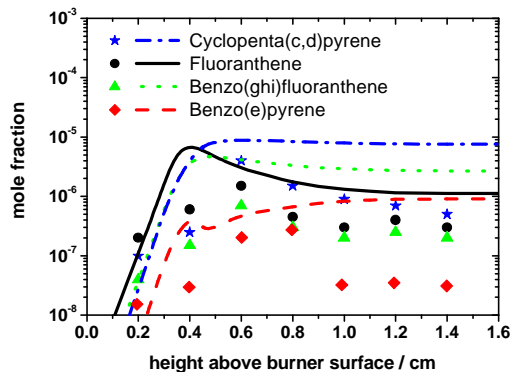


Figure 5: Comparison between model prediction (curves) and experimental data (symbols) for larger PAHs in a premixed laminar atmospheric benzene / air flame, C/O = 0.72 [12].

As mentioned before, the experimental data base for the rate constants and thermodynamic data in the PAH mechanism is extremely poor. Therefore it is not surprising that the prediction of the concentration profiles for larger aromatic species is not presently satisfactory.

### Soot formation

Regarding the prediction of soot particles by mechanistic soot models, coagulation of PAHs is the dominant pathway for particle inception. In this context it is discussed which PAH can start to coagulate: small aromatics such as phenanthrene and pyrene with amu around 200, eventually with reduced coagulation efficiency, or only higher mass PAHs, which were observed at relatively high concentrations, too. Different calculation results showing the influence of a few parameters on the soot yield are shown in figure 6.

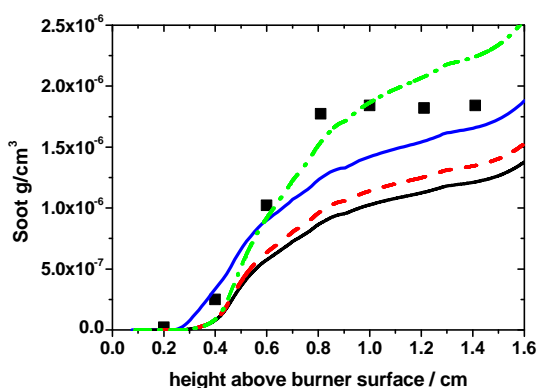


Figure 6: Comparison between model prediction (curves) and experimental data (symbols) for soot concentration in a premixed laminar atmospheric benzene / air flame, C/O = 0.72 [12].

Solid, black curve: Coagulation of all PAHs with amu = 200, soot density  $1.8 \text{ g/cm}^3$ ,  $a = 0.423 = \text{constant}$ . Dashed, red curve: as solid, black curve, but with soot density  $2.0 \text{ g/cm}^3$ . Dash-dotted, green curve: as solid, black curve, but  $a = 1 = \text{constant}$ . Solid, blue curve: as solid, black curve, but with coagulation of all PAHs with amu = 178.

The calculated black curve includes the coagulation of all PAHs with masses more than 200 amu. In the calculation symbolized by the blue curve, polyaromatic species with masses lower 200 amu, namely between 178 and 200 amu like phenanthrene were allowed to coagulate also. This assumption leads to an earlier beginning of the soot formation and results in higher values. For both calculations, the same assumptions were used: (i) a constant soot density  $\rho = 1.8 \text{ g/cm}^3$  and (ii) a constant value of the sticking coefficient  $a = 0.423$  corresponding to the maximum flame temperature of 1850 K, according to the expression from ref. [14]:

$$[\tanh(8168/T_{\text{max}} - 4.57) + 1] / 2.$$

Retaining the preferred coagulation of larger mass species (black curve), the relatively small influence of

assuming a higher soot density of  $2.0 \text{ g/cm}^3$  is shown by the red dashed curve.

The dash-dotted green curve shows the influence of the surface growth reactions on soot concentration: the value for the available surface site ratio was increased to the maximum value of 1. For this assumption, nearly perfect agreement between measured soot mass concentrations and calculated values is achieved in the early soot formation region. For higher height above burner values, the measured soot concentration is over predicted, mainly because the ageing of the soot particles which coincides with a reduction in the available surface site resulting in a smaller value of the sticking coefficient  $a$ , is neglected. Application of a variable decreasing value for the active surface site ratio with particle ageing would result in a better agreement between measured and calculated soot concentrations.

### Stronger sooting benzene/air flame, C/O = 0.77:

For these conditions, the agreement between model calculation and experimental results for different aromatic species (Fig. 7) is not as good as in the less rich premixed flame.

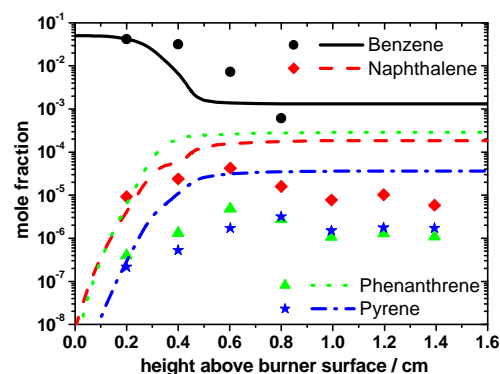


Figure 7: Comparison between model prediction (curves) and experimental data (symbols) for larger mass aromatic species in a premixed laminar atmospheric benzene / air flame, C/O = 0.77 [12].

The prediction of the decrease in benzene concentration is faster than measurement indicates. Assuming an experimental error of 2 mm in the position of the temperature and the concentrations would lead to a nearly perfect agreement between calculated and measured benzene concentration.

The concentration of pyrene is overpredicted, similar to the finding in the slightly sooting flame.

The deviation between model calculation and experimental data is for higher mass PAHs smaller than one order of magnitude (Fig. 8). This is believed to be a very good agreement, considering the high boiling points of the large PAHs and the hereby resulting measurement and detection problems due to condensation of the PAHs during sampling.

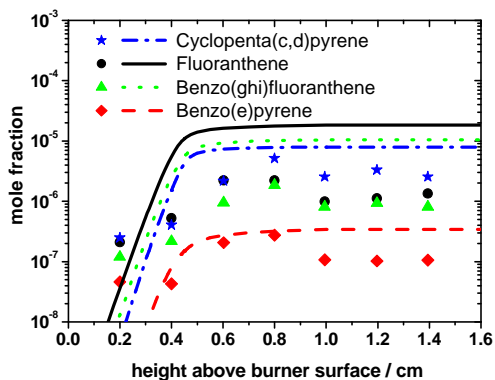


Figure 8: Comparison between model prediction (curves) and experimental data (symbols) for polyaromatic species in a premixed laminar atmospheric benzene / air flame,  $C/O = 0.77$  [12]

In Fig. 9, calculated soot mass concentration profiles are compared with measured data. The onset in the calculation has been shifted by 2 mm, as mentioned above. A soot density  $\rho = 1.8 \text{ g/cm}^3$  and a constant value for  $a = 0.562$ , corresponding to a maximum temperature  $T = 1742 \text{ K}$ , were assumed for the calculations. The simulations which were carried out for phenanthrene or pyrene as the smallest PAH to undergo coagulation show a shape similar to the experimental profile. It has to be pointed out that the absolute values of the predictions are by factors of 2 to 4 smaller than the ones of the experiments.

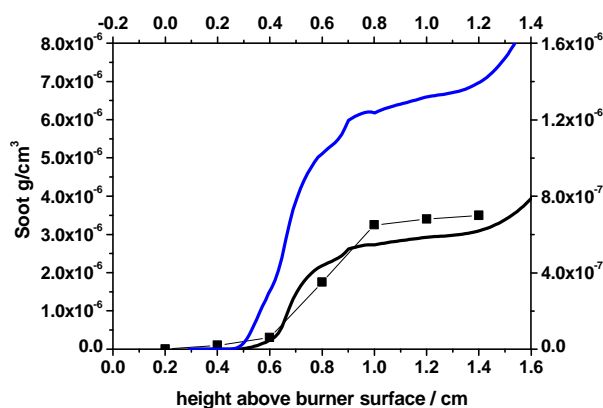


Figure 9: Comparison between model prediction (curves) and experimental data (symbols) for soot concentration in a premixed laminar atmospheric benzene / air flame,  $C/O = 0.77$  [12]. Experimental data: symbols corresponding to left and bottom axis, predicted data corresponding to right and top axis. Solid, black curve: Coagulation of all PAH with masses more than 200 amu (pyrene). Solid, blue curve: as black curve, but with coagulation of all PAHs with amu = 178 (phenanthrene)

## Conclusions

A detailed gas phase reaction mechanism which had been developed in our group was used for the prediction of concentration profiles, in particular of large PAHs, the main soot precursors. The model predictions were compared with experimental data from a laminar premixed benzene air flame at different equivalence ratios. The relatively simple PAH model is able to reproduce dominant PAH species concentrations within one order of magnitude if phenanthrene and pyrene concentrations are predicted within the right order of magnitude.

It has been also demonstrated that the gas phase reaction model, combined with the particle formation module, is able to predict the main features of soot production in a laminar premixed atmospheric benzene flame.

The results of the present work suggest investigations in more detail on the formation routes to larger mass PAHs, performed with tools like single pulse shock tubes or high temperature flow reactors with high temporal resolution and well defined conditions. Thus, the experimental data base could be enlarged considerably attributing to a better understanding of formation and growth of polycyclic aromatic hydrocarbons.

## References

- [1] M. Frenklach and H. Wang, in: H. Bockhorn (Editor), *Soot Formation in Combustion, Mechanisms and Models*, Springer Series in Chemical Physics 59, Springer-Verlag, Berlin, (1994) 165-190.
- [2] H. Böhm, M. Braun-Unkhoff, and P. Frank, *Progress in Computational Fluid Dynamics* 3 (2003) 145-150.
- [3] D. Hu, M. Braun-Unkhoff and P. Frank, *Z. Phys. Chem.* 214 (4) (2000) 473-491.
- [4] H. Wang and M. Frenklach, *Combust. Flame* 110 (1997) 173-221.
- [5] S. J. Harris, A. M. Weiner and R. J. Blint, *Combust. Flame* 72 (1988) 91-109.
- [6] H. Böhm and H. Jander, *Phys. Chem. Chem. Phys.* 1 (1999) 3775-3781
- [7] H. Richter, W. J. Grieco and J. B. Howard, *Combust. Flame* 119 (1999) 1-20.
- [8] K. Roy, C. Horn, P. Frank, V. Slutsky and Th. Just, *Proc. Combust. Inst.* 27 (1998) 329-336.
- [9] S. Scherer, Th. Just and P. Frank, *Proc. Combust. Inst.* 28 (2000) 1511-1518.
- [10] A. D'Anna A. Violi and A. D'Alessio, *Combust. Flame* 121 (2000) 418-429.
- [11] H. Richter, T. G. Benish, O. A. Mazzyar, W. H. Green, J.B. Howard, *Proc. Combust. Inst.* 28 (2000) 2609-2618.
- [12] A. Tregrossi, A. Ciajolo, R. Barbella, *Combustion and Flame* 117 (1999) 553-561.
- [13] R. J. Kee, J. F. Grcar, M. D. Smooke and J. A. Miller, "PREMIX", Sandia National Laboratories, Livermore, CA (USA), Report: SAND85 8240 (1985).
- [14] A. Kazakov, H. Wang, M. Frenklach, *Combustion and Flame* 100 (1995) 111-120.